

Bulk magnetic properties and phase diagram of Li-doped La_2CuO_4 : Common magnetic response of hole-doped CuO_2 planes

T. Sasagawa,^{1,2} P. K. Mang,² O. P. Vajk,³ A. Kapitulnik,^{2,3} and M. Greven^{2,4}

¹*Department of Advanced Materials Science, University of Tokyo, 7-3-1 Hongo, Bunkyo-ku, Tokyo 113-0033, Japan*

²*Department of Applied Physics, Stanford University, Stanford, California 94305*

³*Physics, Stanford University, Stanford, California 94305*

⁴*Stanford Synchrotron Radiation Laboratory, Stanford University, Stanford, California 94305*

(Published: Physical Review B **66**, 184512 (2002))

Although $\text{La}_2\text{Cu}_{1-x}\text{Li}_x\text{O}_4$ (Li-LCO) differs from $\text{La}_{2-x}\text{Sr}_x\text{CuO}_4$ (Sr-LCO) in many ways (e.g., the absence of metallic transport, high- T_c superconductivity, and incommensurate antiferromagnetic correlations), it has been known that certain magnetic properties are remarkably similar. The present work establishes the detailed bulk magnetic phase diagram of Li-LCO ($0 \leq x \leq 0.07$), which is found to be nearly identical to that of lightly-doped Sr-LCO, and therefore extends the universality of the phase diagram to hole-doped but nonsuperconducting cuprates.

PACS numbers: 74.25.Ha, 74.72.Dn, 75.50.Lk

I. INTRODUCTION

Depending on the nature and concentration of dopants, La_2CuO_4 (LCO) displays a wide variety of phenomena such as antiferromagnetism, spin glass (SG) behavior, an anomalous metallic response, and high-temperature superconductivity (HTS). Undoped LCO contains weakly coupled CuO_2 planes and exhibits antiferromagnetic (AF) order of the Cu^{2+} spin-1/2 moments below $T_N \approx 325$ K. Replacement of Cu^{2+} by nonmagnetic Zn^{2+} or Mg^{2+} models random spin dilution, leading the system into a disordered state at doping concentrations above $\sim 40\%$.¹ On the other hand, substitution of divalent alkaline earth cations for La^{3+} or the introduction of excess interstitial oxygen introduces hole charge carriers into the CuO_2 planes which frustrate the spin system.² A concentration of $x = 0.02$ in $\text{La}_{2-x}\text{Sr}_x\text{CuO}_4$ (Sr-LCO) is enough to destroy the AF order; this value is one order of magnitude smaller than for the spin-dilution case. Spin freezing has been found at low temperatures in the AF doping regime ($x < 0.02$),³ with recent direct evidence for electronic phase separation.⁴ Further doping ($x > 0.02$) leads to the emergence of a SG phase,⁵⁻⁷ followed by superconductivity for $x \approx 0.06 - 0.25$. SG order is found to coexist with superconductivity,⁸ with no apparent anomaly in the SG temperature at the doping level $x \sim 0.06$ at which superconductivity first occurs.⁸⁻¹⁰ The phase diagram of the substitutionally-doped bilayer material $\text{Y}_{1-x}\text{Ca}_x\text{Ba}_2\text{Cu}_3\text{O}_6$ (Ca-YBCO) closely resembles that of Sr-LCO,⁹ and spin freezing has also been found in LCO (Ref. 11) and YBCO (Ref. 12) doped with excess oxygen.

The extrapolated disappearance of SG order in Sr-LCO and Ca-YBCO appears to coincide with the doping level at which the normal state pseudogap extrapolates to zero, and it has been suggested that this might be consistent with predictions involving quantum criticality.^{10,13,14} In the d -density wave picture of HTS,¹³

the reason for the lack of a genuine phase transition at the pseudogap temperature is that the disorder present in all existing cuprates corrupts the d -density wave order and transforms the transition into the low-temperature SG transition. While the freezing of d -density wave fluctuations is one proposal for the origin of the SG in doped cuprates, there also exist other interpretations.^{5-7,15-18} For example, it has been argued that the glassiness found in doped Mott insulators may be self-generated, due to the competition between interactions on different length scales, and that quenched disorder may merely further stabilize SG order.¹⁷ The most discussed scenario has been the so-called cluster SG,^{5,6} with holes on the cluster boundaries and in the clusters giving rise to SG physics and to the experimentally observed incommensurate spin correlations.⁷

Given the enormous interest in the connection between magnetic correlations and HTS, it would be valuable to investigate the detailed magnetic properties of related, nonmetallic materials such as $\text{La}_2\text{Cu}_{1-x}\text{Li}_x\text{O}_4$ (Li-LCO).¹⁹⁻²³ Since Li^+ not only provides one hole carrier, but also removes a Cu^{2+} spin, this system experiences the dual effects of spin dilution and frustration. Unlike Sr-LCO, Li-LCO does not superconduct¹⁹ and shows no evidence of incommensurate AF correlations.²³ However, early work on polycrystalline samples reported a rapid suppression of AF order with doping,²⁰⁻²² similar to Sr doping rather than Zn doping, and evidence for spin freezing in the Néel state.²² The remarkable similarity of magnetic properties of lightly doped Li-LCO with those of Sr-LCO has been interpreted as due to new collective behavior of the holes.²² Therefore, in connection with HTS, the detailed magnetic properties and phase diagram of Li-LCO are of considerable interest. Experimentally, spin freezing is observed at a different temperature, depending on the time scale of the probe.^{7,24} Unlike NQR,^{3,22} μSR ,^{9,10} and neutron scattering,^{4,7} magnetometry using a superconducting quantum interference

device (SQUID) is essentially a static probe, allowing a more accurate extraction of the SG transition temperature T_{sg} .^{6,7} Our results for lightly-doped samples demonstrate the feasibility of using bulk magnetometry to extract spin freezing temperatures in the Néel regime. The present magnetometry study establishes the existence of a nearly quantitative agreement of the bulk magnetic phase diagram of Li-LCO with that of Sr-LCO. Since the strength and type of the disorder as well as the charge transport differ significantly in these two materials, this finding places constraints on the origin of the SG degrees of freedom in hole-doped cuprates.

II. EXPERIMENTAL

Using the traveling-solvent floating-zone method,²⁵ we have succeeded in growing large single crystals of $\text{La}_2\text{Cu}_{1-x}\text{Li}_x\text{O}_4$ ($0 \leq x \leq 0.07$). The crystal axes were precisely determined by the x-ray Laue backscattering technique. In order to eliminate possible hole doping by excess oxygen, the crystals were carefully heat treated under reducing conditions. The Li concentrations were estimated to within ± 0.003 from x-ray diffraction measurements of the lattice constants.²¹ For a few samples, we confirmed this estimate using neutron diffraction to determine structural and Néel transition temperatures.²¹ All magnetometry data reported here were taken with a commercial SQUID magnetometer with the magnetic field along the tetragonal a -axis.

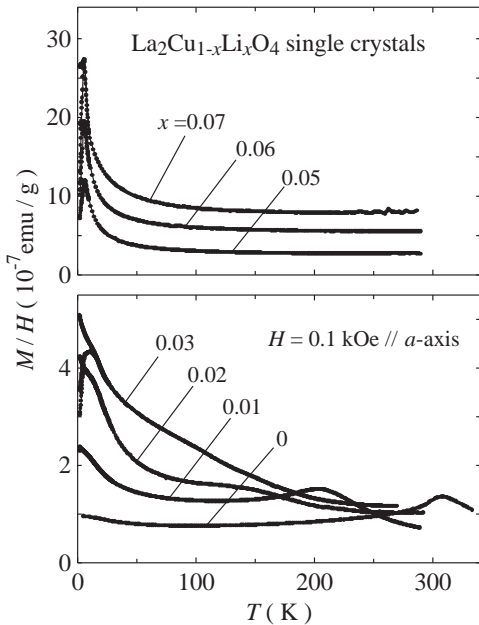


FIG. 1. Magnetic susceptibility of $\text{La}_2\text{Cu}_{1-x}\text{Li}_x\text{O}_4$ with a systematic change of x . A magnetic field $H = 0.1$ kOe was applied parallel to the tetragonal a -axis.

III. RESULTS AND DISCUSSIONS

Figure 1 summarizes the temperature and doping dependence of the magnetic susceptibility of $\text{La}_2\text{Cu}_{1-x}\text{Li}_x\text{O}_4$, taken with a field of $H = 0.1$ kOe along the tetragonal a -axis. The data exhibit several features which systematically shift with doping up to $x = 0.03$, and change their nature above this doping level. Earlier powder studies had demonstrated a rapid suppression of the AF order with Li doping,^{20–22} and the Li concentration at which Néel order is lost corresponds to $x \sim 0.03$. The doping dependence of the Néel temperature determined by local^{20,22} and bulk²¹ magnetic probes agree quite well, and until now this has been the only magnetic phase boundary known in the Li system. However, the present results indicate that the phase diagram in Li-LCO is more complicated than what has been determined from powder samples.

μSR results indicate magnetic order at low temperatures even up to $x \sim 0.10$,²⁰ but bulk magnetization measurements in powder samples only show spin paramagnetism for $x > 0.03$.²¹ The temperature dependent susceptibility for $x > 0.03$ can therefore be expressed by the extended Curie-Weiss formula:

$$\chi(T) = \chi_0 + \frac{C}{(T - \Theta)}, \quad (1)$$

where χ_0 , C , and Θ are the T -independent susceptibility, Curie constant, and Curie-Weiss temperature, respectively. Figure 2 shows $\chi(T)$ for $x = 0.05$. As in the earlier powder report,²¹ paramagnetism is observed in the high temperature regime. A fit to Eq. (1) (solid line in Fig. 2) resulted in $\chi_0 = 2.35 \times 10^{-7}$ emu/g, $C = 7.18 \times 10^{-6}$ emu·K/g, and $\Theta < 0.5$ K. We note that these parameters are roughly comparable with those Sr-LCO: $\chi_0 = 0.4 \times 10^{-7}$ emu/g for $x = 0.04$,⁶ $C = 2-5 \times 10^{-6}$ emu K/g, and $\Theta = 0$ K for $x = 0.03-0.05$.^{6,7}

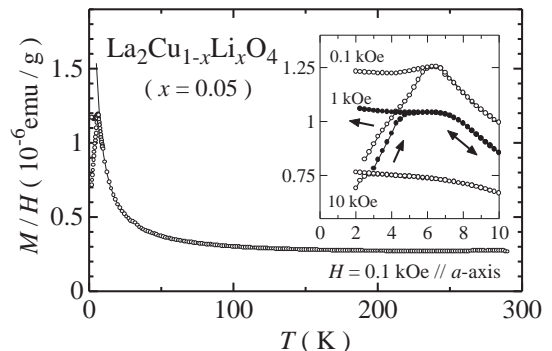


FIG. 2. Magnetic susceptibility of $\text{La}_2\text{Cu}_{0.95}\text{Li}_{0.05}\text{O}_4$. A magnetic field $H = 0.1$ kOe was applied parallel to the tetragonal a -axis. The solid curve is a Curie-Weiss fit of the high-temperature data. The inset shows the low-temperature behavior at various fields. Arrows indicate the T -scan directions.

At low temperatures, $\chi(T)$ deviates significantly from a Curie-Weiss law and shows signatures of a SG. As described in detail below by the appropriate limits of the scaling function, the SG order parameter in the zero-field limit increases from zero upon cooling below T_{sg} , which lead to a decrease of $\chi(T)$ for $T < T_{\text{sg}}$. Furthermore, the resulting peak becomes broader as the applied magnetic field is increased due to the enhancement of the order parameter both above and below T_{sg} . This behavior is demonstrated in the inset of Fig. 2. From the peak in the lowest field ($H = 0.1$ kOe) we determined $T_{\text{sg}} = 6.2(1)$ K, which should be compared to $T_{\text{sg}} = 5.0(5)$ K for Sr-LCO with $x = 0.05$.⁷ Hysteresis below T_{sg} , observed between zero-field-cooled and field-cooled curves, is indicated with the help of arrows in the inset of Fig. 2. Such a behavior is also characteristic of a SG. Observing these features in either small crystals or polycrystalline samples would be difficult because they become obscured as the field is increased, or when the field direction is canted away from the CuO_2 plane.

The large oriented single crystals used in the present study have enabled us to further characterize the SG state by means of a critical scaling analysis of the SG order parameter q , which is experimentally associated with the deviation of the observed equilibrium (field-cooled) susceptibility $\chi(T, H)$ from Curie behavior.²⁶ Normalization to satisfy $0 \leq q \leq 1$ yields

$$q(T, H) = \left[\left(\chi_0 + \frac{C}{T} \right) - \chi(T, H) \right] / \left(\frac{C}{T} \right). \quad (2)$$

Theoretically, the SG transition should obey a scaling relation²⁶ as observed in other critical phenomena. Using the reduced temperature $t = (T - T_{\text{sg}})/T_{\text{sg}}$ and a scaling function $F_{\pm}(z)$, the SG order parameter is defined as

$$q(T, H) = |t|^{\beta} F_{\pm}(H^2/|t|^{\phi}), \quad (3)$$

where β and $\gamma = \phi - \beta$ are the critical exponents characterizing the SG state.²⁶ The behavior of the scaling function $F_{\pm}(z)$ is well known in the following three limits: (i) $F_{+}(z \rightarrow 0) = 0$ ($t > 0$), (ii) $F_{-}(z \rightarrow 0) = \text{const}$ ($t < 0$), and (iii) $F_{\pm}(z \rightarrow \infty) = z^{\beta/\phi}$. Because a relation $q \sim t^{\beta}$ is immediately found from limit (ii), the exponent β can be estimated from the slope in a log-log plot of q (below T_{sg}) versus t in the limit of zero field. Such an analysis is performed in Fig. 3(a), and an estimate of $\beta = 0.7(1)$ is obtained. Similarly, using the limit (iii), the other exponent, ϕ , can be determined from the dependence of q on H^2 at T_{sg} from the relation $q(T_{\text{sg}}, H) = (H^2)^{\beta/\phi}$. The slope in Fig. 3(b) then gives $\beta/\phi = 0.163(5)$ or $\phi = 4.3(8)$.

Now that we have a good estimate of the critical exponents, we can directly test the scaling relation described by Eq. (3). As shown in Fig. 3(c), we obtain excellent scaling. Through the process of getting the best scaling result, shown in Fig. 3(c), the critical exponents have been optimized further: $\beta = 0.78(5)$ and $\gamma = 4.1(5)$.

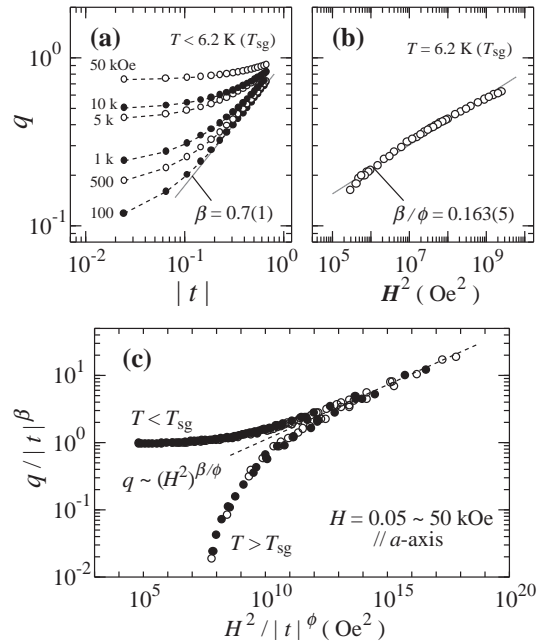


FIG. 3. Scaling analysis of the data in Fig. 1. SG order parameter q as a function of (a) reduced temperature t and (b) field squared H^2 . (c) Scaling plot of the SG order parameter.

The same SG features as for $x = 0.05$ were observed for $x = 0.06$ and 0.07 . The critical exponents obtained in this manner do not depend on x , although T_{sg} decreases with x . We note that, in addition to the comparable values of T_{sg} , the critical exponents are found to be almost identical to those of Sr-LCO,^{6,7} suggesting the existence of the same SG state in both systems. While the observed exponents are consistent with those of canonical SG materials,⁶ we note that recent results for untwinned Sr-LCO crystals reveal unconventional anisotropic behavior.²⁷

For $x < 0.03$, the magnetic susceptibility differs from that for $x > 0.03$. Data for $x = 0.02$ are shown in Fig. 4(a). Two magnetic anomalies are present. One is a high-temperature cusp associated with the AF transition which has already been observed in powder samples.²¹ As shown in Fig. 4(b), neutron data complement the SQUID observations, providing unambiguous evidence of a well-defined Néel transition around this high-temperature bump. We have confirmed the development of the antiferromagnetic peak at the (1,0,0) position (orthorhombic notation) just below the susceptibility anomaly, and determined the Néel temperature to be $T_{\text{N}} = 135$ K. The second anomaly, recognized well below T_{N} , appears somewhat analogous to the SG behavior found for $x > 0.03$ in that we find hysteresis below the anomaly and the onset temperature of magnetic irreversibility is comparable to T_{sg} for $x > 0.03$. Neutron characterization furthermore revealed a sharp structural transition from the tetragonal to orthorhombic phase at 490 K, consistent with a doping level of $x = 0.02$.²¹ This indicates that

our samples have a high degree of chemical homogeneity, and that the observed magnetic anomaly is intrinsic to the $x = 0.02$ phase. Local-probe ^{139}La -NQR and μSR experiments have reported a corresponding spin-freezing within the AF state in Sr-LCO (Refs. 3 and 9) and Li-LCO.²² This has been ascribed to the continuous freezing of the spins of the doped holes on the antiferromagnetic background,³ with independent ordering of Cu^{2+} spins and doped holes,⁹ or due to a collective hole behavior.²² However, to the best of our knowledge, this spin freezing has not been reported thus far from bulk magnetometry for the cuprates. Because the SG behavior is very sensitive to the dopant concentration (x -dependence will be discussed later) and to the field direction, the success of the present observations depended greatly on high-quality single crystals as well as extended measurements in the low-temperature region.

Although the second anomaly appears to be a SG transition, further characterization in terms of critical scaling analysis is not possible due to the ambiguity in the definition of the SG order parameter. Nevertheless, it would be worthwhile to determine a characteristic freezing temperature, T_f . We define T_f as the lower-temperature “shoulder” of the zero-field-cooled data at low H , which corresponds to the onset of magnetic hysteresis for $x = 0.02$, as seen in the inset of Fig. 4(a). We note that, although not shown here, a change in the imaginary part of the ac susceptibility was also observed at this temperature, which can be associated with the drastic change of the spin response due to the onset of the spin freezing.

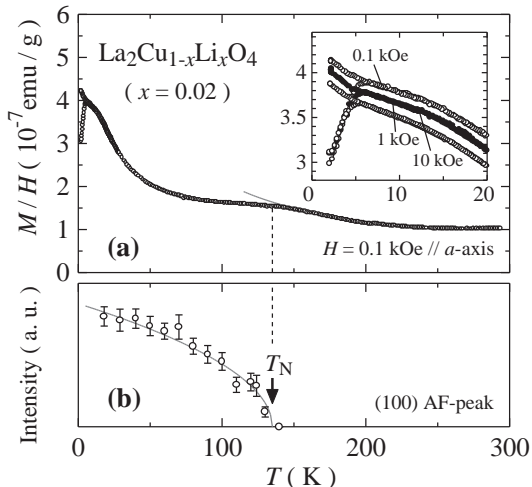


FIG. 4. (a) $\chi(T)$ of $\text{La}_2\text{Cu}_{0.98}\text{Li}_{0.02}\text{O}_4$ as a function of temperature under $H = 0.1$ kOe. The inset magnifies the low-temperature behavior at various fields. (b) T -dependence of the integrated intensity of the (1 0 0) antiferromagnetic neutron peak (orthorhombic notation). The power-law fit (solid curve) gives $T_N = 135$ K, which corresponds well to the cusp in the susceptibility.

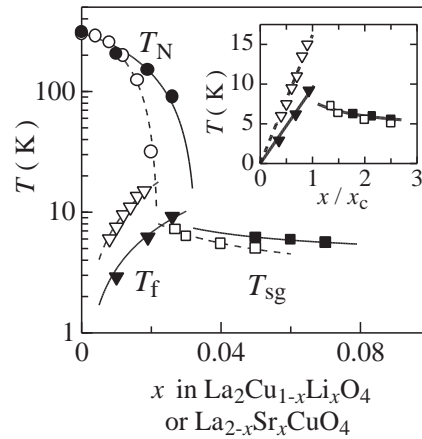


FIG. 5. Magnetic phase diagram for $\text{La}_2\text{Cu}_{1-x}\text{Li}_x\text{O}_4$ (filled symbols) and $\text{La}_{2-x}\text{Sr}_x\text{CuO}_4$ (open symbols; from NQR ($x < 0.02$)³ and magnetometry ($x > 0.02$)⁷): circles for the Néel temperature T_N , triangles for the onset of the SG-like anomaly T_f , and squares for the SG temperature T_{sg} . Inset: scaled phase diagram.

Our results yield the phase diagram summarized in Fig. 5. NQR ($x < 0.02$) (Ref. 3) and magnetometry ($x > 0.02$) (Ref. 7) data from Sr-LCO single crystals are included for comparison. Despite the different nature of the dopants, the phase boundaries for these two compounds are almost identical. Figure 5 demonstrates that $T_f \sim x$ as in Sr-LCO, opposite to the trend with doping for either T_N or T_{sg} . We find $T_f = (339 (14) \text{ K}) \times x$, as compared to $T_f \approx (815 \text{ K}) \times x$ for Sr-LCO from ^{139}La NQR.³

The dopant concentrations at which Néel order is lost in the two materials differ by a factor of $\sim 2/3$. Qualitatively, this shift of the phase boundaries can be understood to result from reduced magnetic frustration in the Li-doped system.²⁸ As shown in the inset of Fig. 5, when normalized by that factor, T_{sg} for Li-LCO ($x > 0.03$) *quantitatively* agrees with the SG temperature for Sr-LCO. Since NQR and magnetometry probe very different time scales, systematic Sr-LCO magnetometry data for $x < 0.02$ would be very desirable for a proper quantitative comparison at low doping.

Recent neutron scattering results reveal direct evidence for electronic phase separation in Sr-LCO ($x < 0.02$) into regions with hole concentrations ≈ 0 and ≈ 0.02 .⁴ The latter phase exhibits diagonal stripes.⁷ Spin freezing occurs below the doping-independent phase separation temperature $T_{ps} \approx 30$ K determined from neutron scattering,⁴ and consistent with previous NQR results.³ For Li-LCO, on the other hand, commensurate AF correlations have been both predicted²⁹ and observed,²³ consistent with the expected stronger pinning potential of the in-plane dopant Li^+ . Consequently, the cluster model, originally proposed for Sr-LCO, but which predicts commensurate AF correlations, might more accurately describe the physics of the Li-doped variant.¹⁶

This model predicts $k_B T_f \sim J_{\text{eff}} x$, where J_{eff} is the effective in-plane exchange coupling constant.¹⁶ While this linear doping dependence is indeed consistent with our observations, the same behavior is found in Sr-LCO.³ On the other hand, it has been speculated that T_f in Sr-LCO might depend linearly on the volume fraction of the SG phase.⁴ The close analogy between the NQR (Refs. 3 and 22) and bulk magnetic properties of the two materials suggests that Li-LCO might phase separate as well.

At higher hole concentrations, the behavior of the carriers differs significantly between Li-LCO and Sr-LCO. The latter material shows an insulator to metal transition and HTS, while the former remains insulating. What is particularly interesting from our present observations is that, in spite of the great difference in charge dynamics for $x > 0.03$, the spin degrees of freedom measured via magnetometry are remarkably similar in both compounds. Both materials show a spin glass transition, with comparable transition temperatures at the same doping value and with the same critical exponents. The values of $T_{\text{sg}}(x)$ for the more disordered material Li-LCO lie above those of Sr-LCO. The relative shift of the SG phase boundaries likely results from an effective decrease of magnetic frustration due to the presence of nonmagnetic Li^+ in Li-LCO.²⁸ In this context, it is worth noting that the magnetic phase boundaries in the double-layer cuprates^{9,10} lie above those of both Li-LCO and Sr-LCO. While differences in the strength and type of disorder might play a subtle role in setting the temperature scales for Néel and SG order, we believe that the predominant effect is the difference in the effective three-dimensional AF coupling between single- and double-layer materials. Specifically, while the interplanar AF coupling is nearly frustrated in doped LCO, this is not the case for the double-layer materials. On the other hand, the relative insensitivity of the low-temperature magnetic phase boundaries of the structurally identical materials Li-LCO and Sr-LCO to the type and strength of the quenched disorder is consistent with the notion that the glassiness in these doped Mott insulators is primarily self-generated.¹⁷

IV. CONCLUSION

The bulk magnetic properties of Li-LCO single crystals are found to be richer than previously reported from powder samples. Our results demonstrate the feasibility of extracting low-temperature freezing temperatures in the Néel state from magnetometry, and call for similar measurements in other cuprates for a proper quantitative comparison. We find that $T_f \sim x$, which also has been reported for Sr-LCO. Since the spin freezing in the latter material occurs in a phase separated state, the close similarity between the doping dependence of the freezing temperature suggests that lightly doped Li-LCO might phase separate as well, despite the stronger pinning potential of the in-plane dopant Li^+ . Outside of the Néel

phase, the spin glass phase boundaries differ by a mere scale factor for the effective doping level. The experimental results for Li-LCO obtained here extend the universality of the bulk magnetic phase diagram to hole-doped but non-superconducting cuprates.

ACKNOWLEDGMENTS

We thank D. Fisher, H. Eisaki, K. Kishio, R.S. Markiewicz, Ch. Niedermayer, C. Panagopoulos, and H. Takagi for fruitful discussions. P.K.M., O.P.V., and M.G. would like to thank the staff of the NIST Center for Neutron Research for their warm hospitality. The work at Stanford was supported by the U.S. DOE under Contract Nos. DE-FG03-99ER45773 and DE-AC03-76SF00515, by NSF CAREER Award No. DMR-9985067, and by the A.P. Sloan Foundation. T.S. was partially supported by JSPS.

-
- ¹ O. P. Vajk, P. K. Mang, M. Greven, P. M. Gehring, and J. W. Lynn, *Science* **295**, 1691 (2002).
 - ² A. Aharony, R. J. Birgeneau, A. Coniglio, M. A. Kastner, and H. E. Stanley, *Phys. Rev. Lett.* **60**, 1330 (1988).
 - ³ F. C. Chou, F. Borsa, J. H. Cho, D. C. Johnston, A. Lascialfari, D. R. Torgeson, and J. Ziolo, *Phys. Rev. Lett.* **71**, 2323 (1993); F. Borsa, P. Carretta, J. H. Cho, F. C. Chou, Q. Hu, D. C. Johnston, A. Lascialfari, D. R. Torgeson, R. J. Gooding, N. M. Salem, and K. J. E. Vos, *Phys. Rev. B* **52**, 7334 (1995).
 - ⁴ M. Matsuda, M. Fujita, K. Yamada, R. J. Birgeneau, Y. Endoh, and G. Shirane, *Phys. Rev. B* **65**, 134515 (2002).
 - ⁵ J. H. Cho, F. Borsa, D. C. Johnston, and D. R. Torgeson, *Phys. Rev. B* **46**, 3179 (1992).
 - ⁶ F. C. Chou, N. R. Belk, M. A. Kastner, R. J. Birgeneau, and A. Aharony, *Phys. Rev. Lett.* **75**, 2204 (1995).
 - ⁷ S. Wakimoto, S. Ueki, Y. Endoh, and K. Yamada, *Phys. Rev. B* **62**, 3547 (2000).
 - ⁸ H. Kitazawa, K. Katsumata, E. Torikai, and K. Nagami, *Solid. State. Commun.* **67**, 1191 (1988); A. Weidinger, Ch. Niedermayer, A. Golnik, R. Simon, E. Recknagel, J. I. Budnick, B. Chamberland, and C. Baines, *Phys. Rev. Lett.* **62**, 102 (1989).
 - ⁹ Ch. Niedermayer, C. Bernhard, T. Blasius, A. Golnik, A. Moodenbaugh, and J. I. Budnick, *Phys. Rev. Lett.* **80**, 3843 (1998).
 - ¹⁰ C. Panagopoulos, B. D. Rainford, J. R. Cooper, and C. A. Scott, *Physica (Amsterdam)* **341C**, 843 (2000); C. Panagopoulos, J. L. Tallon, B. D. Rainford, T. Xiang, J. R. Cooper, and C. A. Scott, *Phys. Rev. B* **66**, 064501 (2002).
 - ¹¹ V. Yu. Pomjakushin, V. N. Duginov, A. A. Zakharov, A. N. Ponomarev, A. Amato, F. N. Gygax, A. Schenck, and D. Herlach, *Physica (Amsterdam)* **272C**, 250 (1996).
 - ¹² R. F. Kiefl, J. H. Brewer, J. Carolan, P. Dosanjh, W. N.

- Hardy, R. Kadono, J. R. Kempton, R. Krahn, P. Schleger, B. X. Yang, Hu Zhou, G. M. Luke, B. Sternlieb, Y. J. Uemura, W. J. Kossler, X. H. Yu, E. J. Ansaldo, H. Takagi, S. Uchida, and C. L. Seaman, *Phys. Rev. Lett.* **63**, 2136 (1989).
- ¹³ S. Chakravarty, R. B. Laughlin, D. K. Morr, and C. Nayak, *Phys. Rev. B* **63**, 094503 (2001).
- ¹⁴ S. Andergassen, S. Caprara, C. Di Castro, and M. Grilli, *Phys. Rev. Lett.* **87**, 056401 (2001), and references therein.
- ¹⁵ V. J. Emery and S. A. Kivelson, *Physica (Amsterdam)* **209C**, 597 (1993); S. A. Kivelson and V. J. Emery, *cond-mat/9809082* (unpublished).
- ¹⁶ R. J. Gooding, N. M. Salem, R. J. Birgeneau, and F. C. Chou, *Phys. Rev. B* **55**, 6360 (1997).
- ¹⁷ J. Schmalian and P. G. Wolynes, *Phys. Rev. Lett.* **85**, 836 (2000); H. Westfahl, Jr., J. Schmalian, and P. G. Wolynes, *Phys. Rev. B* **64**, 174203 (2001).
- ¹⁸ N. Hasselmann, A. H. Castro Neto, and C. Morais Smith, *Europhys. Lett.* **56**, 870 (2001).
- ¹⁹ M. A. Kastner, R. J. Birgeneau, C. Y. Chen, Y. M. Chiang, D. R. Gabbe, H. P. Jenssen, T. Junk, C. J. Peters, P. J. Picone, Tineke Thio, T. R. Thurston, and H. L. Tuller, *Phys. Rev. B* **37**, 111 (1988).
- ²⁰ L. P. Le, R. H. Heffner, D. E. MacLaughlin, K. Kojima, G. M. Luke, B. Nachumi, Y. J. Uemura, J. L. Sarrao, and Z. Fisk, *Phys. Rev. B* **54**, 9538 (1996).
- ²¹ J. L. Sarrao, D. P. Young, Z. Fisk, E. G. Moshopoulou, J. D. Thompson, B. C. Chakoumakos, and S. E. Nagler, *Phys. Rev. B* **54**, 12014 (1996).
- ²² B. J. Suh, P. C. Hammel, Y. Yoshinari, J. D. Thompson, J. L. Sarrao, and Z. Fisk, *Phys. Rev. Lett.* **81**, 2791 (1998).
- ²³ W. Bao, R. J. McQueeney, R. Heffner, J. L. Sarrao, P. Dai, and J. L. Zarestky, *Phys. Rev. Lett.* **84**, 3978 (2000); W. Bao and J. L. Sarrao, *cond-mat/0203318* (unpublished).
- ²⁴ R. S. Markiewicz, F. Cordero, A. Paolone, and R. Cantelli, *Phys. Rev. B* **64**, 054409 (2001), and references therein.
- ²⁵ T. Sasagawa, K. Kishio, Y. Togawa, J. Shimoyama, and K. Kitazawa, *Phys. Rev. Lett.* **80**, 4297 (1998); T. Sasagawa, Y. Togawa, J. Shimoyama, A. Kapitulnik, K. Kitazawa, and K. Kishio, *Phys. Rev. B* **61**, 1610 (2000).
- ²⁶ A.P. Malozemoff, S.E. Barnes, and B. Barbara, *Phys. Rev. Lett.* **51**, 1704 (1983); B. Barbara, A.P. Malozemoff, and Y. Imry, *ibid.* **47**, 1852 (1981).
- ²⁷ A. N. Lavrov, Y. Ando, S. Komiya, and I. Tsukada, *Phys. Rev. Lett.* **87**, 017007 (2001)
- ²⁸ I.Ya. Korenblit, A. Aharony, and O. Entin-Wohlman, *Phys. Rev. B* **60**, 15017 (1999).
- ²⁹ C. Buhler, S. Yunoki, and A. Moreo, *Phys. Rev. B* **62**, 3620 (2000).